Biogeosciences Discuss., 11, 2537–2568, 2014
www.biogeosciences-discuss.net/11/2537/2014/
doi:10.5194/bgd-11-2537-2014

Biogeosciences Discussions Open Access

Tree-ring responses to extreme climate events as benchmarks for terrestrial dynamic vegetation models

A. Rammig[1], M. Wiedermann[1,2], J. F. Donges[1,3], F. Babst[4], W. von Bloh[1], D. Frank[5,6], K. Thonicke[1], and M. D. Mahecha[7,8]

[1]Earth System Analysis, Potsdam Institute for Climate Impact Research, Telegraphenberg A62, 14412 Potsdam, Germany
[2]Department of Physics, Humboldt University, Newtonstr. 15, 12489 Berlin, Germany
[3]Stockholm Resilience Centre, Stockholm University, Kräftriket 2B, 114 19 Stockholm, Sweden
[4]Laboratory of Tree-Ring Research, University of Arizona, 1215 E Lowell St, Tucson AZ 85721, USA
[5]Swiss Federal Research Institute WSL, Zürcherstr. 111, 8903 Birmensdorf, Switzerland
[6]Oeschger Centre for Climate Change Research, University of Bern, Zähringerstrasse 25, 3012 Bern, Switzerland
[7]Max Planck Institute for Biogeochemistry, Hans-Knöll-Str. 10, 07745 Jena, Germany
[8]German Centre for Integrative Biodiversity Research (iDiv) Halle-Jena-Leipzig, Deutscher Platz 5e, 04103 Leipzig, Germany

Received: 28 January 2014 – Accepted: 31 January 2014 – Published: 12 February 2014

Correspondence to: A. Rammig (anja.rammig@pik-potsdam.de)

Published by Copernicus Publications on behalf of the European Geosciences Union.

Abstract

Climate extremes can trigger exceptional responses in terrestrial ecosystems, for instance by altering growth or mortality rates. Effects of this kind are often manifested in reductions of the local net primary production (NPP). Investigating a set of European long-term data on annual radial tree growth confirms this pattern: we find that 53 % of tree ring width (TRW) indices are below one standard deviation, and up to 16 % of the TRW values are below two standard deviations in years with extremely high temperatures and low precipitation. Based on these findings we investigate if climate driven patterns in long-term tree growth data may serve as benchmarks for state-of-the-art dynamic vegetation models such as LPJmL. The model simulates NPP but not explicitly the radial tree ring growth, hence requiring a generic method to ensure an objective comparison. Here we propose an analysis scheme that quantifies the coincidence rate of climate extremes with some biotic responses (here TRW or simulated NPP). We find that the reduction in tree-ring width during drought extremes is lower than the corresponding reduction of simulated NPP. We identify ten extreme years during the 20th century in which both, model and measurements indicate high coincidence rates across Europe. However, we detect substantial regional differences in simulated and observed responses to extreme events. One explanation for this discrepancy could be that the tree-ring data have preferentially been sampled at more climatically stressed sites. The model-data difference is amplified by the fact that dynamic vegetation models are designed to simulate mean ecosystem responses at landscape or regional scale. However, we find that both model-data and measurements display carry-over effects from the previous year. We conclude that using radial tree growth is a good basis for generic model-benchmarks if the data are analyzed by scale-free measures such as coincidence analysis. Our study shows strong reductions in carbon sequestration during extreme years. However, for a better understanding of the impact of extreme events on e.g. the long-term fate of the European carbon balance, more long-term measurement data and improved process-based models are needed.

1 Introduction

Extreme climate events are known to trigger exceptional responses in terrestrial ecosystems (Reyer et al., 2012; Smith, 2011; Zscheischler et al., 2014b, a). The question, which ecosystem processes exceed their natural range of variability in the wake of environmental extremes is of paramount importance for anticipating the fate of land ecosystems under climate change scenarios (Cotrufo et al., 2011; Jentsch et al., 2011). This knowledge is important because ecosystem response e.g. to drought events (Schwalm et al., 2012) may decrease the economic returns from forest ecosystems (Hanewinkel et al., 2013) or lead to substantial net CO_2 emissions and amplify climate change (Reichstein et al., 2013). One prominent example is the 2003 heat wave in Europe that alone caused carbon emissions of $\sim 0.5\,\mathrm{Pg\,C\,yr^{-1}}$ from forests that usually act as carbon sinks (Ciais et al., 2005; Janssen et al., 2003). However, it is important to note that extreme events may have differential effects in different biomes, e.g. enhanced vegetation growth during the 2003 heat wave at high elevations in the Alps (Jolly et al., 2005).

In many low- and mid-latitude areas, water stress and high temperatures reduce evapotranspiration and productivity (Granier et al., 2007). Yet, the general applicability of such studies is challenged by different climate responses of forests across biomes and tree species (Babst et al., 2013b; Granier et al., 2007; Lindner et al., 2010). Increasing amounts of atmospheric CO_2 may serve as a buffer against drought by enhancing water use efficiency (e.g. Andreu-Hayles et al., 2011; Penuelas et al., 2011; Keenan et al., 2013), but again the strength of these effects is poorly constrained and may differ among tree species or tree age classes (Gedalof and Berg, 2010), and likewise depend on nutrient availability (e.g. Norby et al., 2010). Another known, yet understudied aspect, is the role of "lagged effects", i.e. when previous year's extremes influence forest productivity e.g. via decreased non-structural carbohydrate reserves (e.g. Dietze et al., 2013; Fritts, 1976; Richardson et al., 2013) or via altered mortality rates (Bréda et al., 2006; Moreno et al., 2013). Carbon sequestered in the second half

of the growing season is generally not used for radial growth but supports a combination of cell-wall thickening and storage (Babst et al., 2013a). This effect is often visible in tree-ring data as a positive relationship with previous fall climate (Wettstein et al., 2011). Depending on their sign, climate anomalies in this season may thus enhance or mitigate the impact of extremes on forest growth in the subsequent year, because they directly affect the growing season length and the related replenishment of carbon storage (Kuptz et al., 2011). Also the interaction of carbon accumulation with seed production (i.e. mast years) may sometimes lead to low growth events regardless of climatic conditions, thus putting certain restrictions on using stem growth alone as proxy for total biomass production (Mund et al., 2010).

Overall, the impacts of extreme events under current and past conditions remain insufficiently documented. This is a natural consequence of the low occurrence probability of the events accompanied by chronically scarce observations (Innes, 1998; Smith, 2011). Hence, it is difficult to predict impacts of expected increases of extreme events (Barriopedro et al., 2011; Field et al., 2012) on the terrestrial carbon cycle (Reichstein et al., 2013). In this context terrestrial biosphere models play a crucial role for quantifying the impact of climate extremes on the terrestrial carbon cycle, most importantly on the net primary productivity (NPP, Keenan et al., 2012). One prerequisite is, however, that models are well tested for their capacity to reproduce the relevant signatures of extreme impacts in the recent past. These models simulate carbon accumulation in different plant compartments such as root, stem and leaves. Annual variation and impacts of extreme events are in these models reflected best by NPP.

One critical issue is identifying suitable benchmarks for testing terrestrial biosphere models as suggested for average climate conditions (Dalmonech and Zaehle, 2013; Kelley et al., 2013; Luo et al., 2012). There is, however, a lack of process understanding in biosphere models amplified by data paucity to benchmark model performance under extreme conditions. Annual radial growth increments (tree-ring chronologies) are increasingly understood as a valuable long-term observational reference offering one of the few opportunities to quantify ecosystem responses on time-scales sufficient to

observe multiple extreme events (Babst et al., 2012). With certain restrictions, tree-ring chronologies can be interpreted as long-term proxies for the variability of stand-scale productivity and thus offer a possibility to relate long-term tree growth to climate fluctuations at regional and continental scale and to quantify the impact of single extreme years (e.g. Babst et al., 2012; Battipaglia et al., 2010).

In this study, we propose a generic method to evaluate dynamic vegetation models in relation to tree ring chronologies by exploiting the coincidence of extremes in tree ring width (TRW) and climate variables in long (> 50 yr) time series. This analysis framework is based on the general method of coincidence analysis that was put forward by Donges et al. (2011) in a different context and is in the present study tailored to address the following question:

- Do state-of-the-art dynamic vegetation models agree with observed responses to climate extremes?
- How can long-term observations help us understanding biotic responses to extreme events?

The goal of our study is to benchmark dynamic vegetation models regarding their response to extreme climate events by using long-term observations of tree-ring width. In our study, we focus on the biotic response to drought and heat events. We first compare the reductions in tree-ring width indices (TRW) and simulated NPP during climatic extremes, thereby acknowledging that TRW and simulated NPP may respond differently to the considered climate extremes. Climate extremes may not be the only driver for anomalous behavior of TRW but also disturbances, such as insect outbreaks or fire, forestry management and lag effects play an important role (e.g. Franke et al., 2013). These drivers are, except for fire, not included in our model simulations. On the other hand, simulated NPP integrates different effects than visible in tree ring records and responds more directly to climate extremes. Thus, our generic approach for comparison seems suitable and will contribute to an increased process understanding. We do therefore not directly compare extreme responses in TRW with simulated NPP but

rather search for possible causal relationships between climate extremes and TRW and between climate extremes and simulated NPP. We systematically evaluate observed and simulated responses to climate extremes by analyzing regional response patterns and identifying years with strong responses to extreme events. We also consider instantaneous and lagged effects of climate extremes on forest growth in the analysis. The present study advances the quantification of sensitivity of forest growth to climate extremes and provides suggestions for biosphere model improvement.

2 Material and methods

2.1 Observed and modeled data

2.1.1 Measurements of tree ring widths

We used tree ring width index (TRW) chronologies from 606 sites across Europe and parts of Northern Africa (10° W–40° E, 30–70° N). These data represent a subset of the European tree-ring network (Babst et al., 2013b) which includes measurements from 36 tree species. For the purpose of this study, we grouped sites into three categories: common needle-leaved species (e.g. *Larix decidua, Picea abies, Pinus Syvestris, Abies alba*; 116 sites), broadleaved species (e.g. *Fagus silvatica, Quercus robur, Quercus petraea*; 378 sites) and other species (mainly Mediterranean conifers; 112 sites). For the detection of growth extremes, low frequency variability including the biological age/size trend characteristic for tree-ring data was removed from the constituent tree-ring time-series at each site using a spline detrending with a 50 % frequency cutoff response at 30 yr (Babst et al., 2012). Prior to detrending, the variance of each time-series was modified using an adaptive power transformation as described by Cook & Peters (1997) and the mean of the tree-ring data corrected for changes in sample replication (Frank et al., 2007) to reduce biases in the detection of growth extremes induced by variance changes throughout the tree-ring chronologies. The tree-

ring detrending and standardization procedure converts the tree-ring width data into dimensionless indices (so-called tree-ring width indices, TRW) with a mean of approximately unity. The tree ring dataset spans most of terrestrial Europe, but is not evenly distributed across the continent (see Babst et al., 2013b and Fig. 3). Conifer sites are most frequent in Scandinavia, in the Alpine region, and in the Mediterranean, while broadleaved species are predominantly located in Central Europe and Northern Spain (Babst et al., 2013b).

2.1.2 Climate data

We use the WATCH-ERA-Interim daily climate data at 0.25 latitude/longitude resolution based on down-scaled WATCH climate data (Weedon et al., 2011) for the years 1901–2001 and extended to 2010 using downscaled ERA-Interim climate data (Dee et al., 2011). Daily temperature, precipitation and solar radiation were used to drive the model runs. For the coincidence analysis with TRW and simulated NPP, we calculate annually average temperature (T) and sums of precipitation (P) over the growing season from the climate data set (see below).

2.1.3 Simulated net primary productivity (NPP)

Simulations of monthly NPP are performed with the dynamic global vegetation model LPJmL (Bondeau et al., 2007; Sitch et al., 2003) with a fully coupled carbon and water cycle (Gerten et al., 2004). The model is driven by temperature, radiation, precipitation and atmospheric CO_2 concentration. Productivity of vegetation (GPP) for each plant functional type (PFT) is simulated by a process-based photosynthesis scheme based on Farquhar (Farquhar et al., 1980) that adjusts carboxylation capacity and leaf nitrogen seasonally and within the canopy profile (Haxeltine and Prentice, 1996). Net primary production (NPP) is derived by subtracting maintenance and growth respiration from GPP. LPJmL simulates the allocation of accumulated carbon to the plant's compartments (leaves, stem, root and reproductive organs) according to allometric

constraints. Responses of the modeled vegetation to climate extremes include the inhibition of photosynthesis and increased maintenance respiration at high temperatures, and reduced stomatal conductance and thus reduced photosynthesis with water stress.

For the present study, we ran LPJmL in its natural vegetation mode not considering land management and land-use change. Process-based simulation of fire is included by the SPITFIRE model which is coupled to LPJmL (Thonicke et al., 2010). Simulation runs were performed at 0.25° × 0.25° degree spatial resolution based on the WATCH-ERA-Interim daily climate data. A global value of annual atmospheric CO_2 concentration was prescribed for the 1901–2010 period based on NOAA-ESRL (2013). The transient runs from 1901 to 2010 were preceded by a spin-up of 1000 yr using 30 yr of the climate drivers in order to obtain equilibrium carbon pools and fluxes and vegetation cover. Model parameterization and soil types were as in Gerten et al. (2004) and Sitch et al. (2003).

2.1.4 Determination of the growing season for TRW and simulated NPP

To determine the length of the growing season (GS_{obs}) for each tree ring site, we use the fraction of photosynthetically absorbed radiation derived from remote sensing and interpolated to daily values (FAPAR from MODIS, Pinty et al., 2011). We constrain GS_{obs} based on a mixture of absolute and relative heuristic criteria. First, we flagged days as no growing season where FAPAR values drop below 0.12 or are below −0.8 standard deviations of FAPAR. To ensure that the second criterion does not affect evergreen sites, we reset all values > 0.43 to growing season. We then searched for the connected phases of GS_{obs}, but used the restriction that the minimum duration of GS_{obs} is one month. Note that we only allow for one single GS_{obs} in Europe, as we assume that double growing seasons do not play a substantial role. The dynamic definitions of the GS_{obs} derived from FAPAR allow for adjustment of the growing seasons to the effective local conditions; these local GS_{obs} were used for the determination of coincidences of climate extremes during the growing season and in the tree ring data.

To determine the length of the growing season for each simulated grid cell (GS_{sim}), we use the simulation results for NPP. As GS_{sim} we define here the longest period of subsequent months per year with monthly NPP > 0.

2.1.5 Preprocessing of climate data, TRW and simulated NPP for coincidence analysis

The coincidence analysis requires pairing each point in the TRW dataset with local *T* and *P* variability. Accordingly, each TRW site is associated with the site-specific (i.e., geographically encompassing) climate grid cell of the WATCH-ERA-Interim data at 0.25° × 0.25° spatial resolution. By doing so, we obtain 606 pairs of time-series representing tree-ring growth and climatological data. Monthly temperature and precipitation data are averaged and summed, respectively, over the growing season (see Sect. 2.1.5). The maximum temporal overlap between each pair of time series determines the length of the period for coincidence analysis.

To obtain pairs of time-series for the comparison of simulated NPP with *P* and *T* in a comparable way as for TRW, we calculate the sum of simulated NPP over the growing season (see Sect. 2.1.5). Analogously to the coincidence analysis between TRW and climate data we again compute the average temperature and total precipitation over the growing season, where NPP > 0. We obtain pairs of simulated NPP and climate drivers for each grid cell.

The TRW data set consists of 606 time series at selected measurement sites throughout Europe. For comparison with simulated NPP, we select the corresponding grid cells centers nearest to the measurement sites.

2.2 Coincidence analysis and definition of extreme events

For our analysis, we search for coincidences (Donges et al., 2011) between specific percentiles in the pairs of biotic and climate time series. In the case of TRW and NPP, values smaller than the 10th percentiles were used (low-productivity extremes). In the

climate records, all values exceeding the 90th percentiles of mean growing season temperature (hot extremes) and being less than the 10th percentile of the total growing season precipitation (dry extremes) were defined as extreme events. This combination of climatic and biotic extremes implicitly tests the link between extremely high temperature or low precipitation in causing low growth responses at all sites. At alpine or boreal sites, particularly high temperatures may even lead to better growth conditions (e.g. Jolly et al., 2005). Similarly, extremely low temperatures during the growing season could cause low growth extremes, e.g. in the Alps or the boreal zone (e.g. Babst et al., 2012). We therefore carefully interpret our results regarding these issues. The method of coincidence analysis would also allow for evaluating other types of extremes but this is out of the scope of the present paper.

To obtain the number of coincidences, K, between two given time series, we count the number of extreme events that both time series have in common simultaneously or allowing for a predefined lag. For the determination of K there are two parameters in the coincidence analysis: (1) Δt determines the width of the time window (in years, y) in which a TRW or NPP extreme can fall after a T or P extreme. For $\Delta t = 1y$ only coincidences between TRW or NPP with T or P during one year are counted. For $\Delta t = 2y$, coincidences between TRW or NPP with T or P during a time window of two years are counted, all coincidences falling in this time window are counted as $K = 1$. (2) tau determines the time lag between the TRW or NPP extreme and the T or P extreme. We distinguish $\Delta t = 1y$ and tau $= 0y$ (which account for coincidences occurring in the same year, i.e. instantaneous growth responses) and $\Delta t = 1y$ and tau $= 1y$ to investigate lagged effects, i.e. extreme growth responses in the following year (Fig. 1 and see also Donges et al., 2011). We then normalize K by the total number of extreme events N in the climate time-series of T or P to obtain the coincidence rate r with $0 \leq r \leq 1$ (0 if no coincidences occur and 1 if the maximum number of possible coincidences occurs).

2.3 Testing the significance of coincidences

Autocorrelations as well as the specific shape of the distribution of amplitudes in the considered climatological and biotic time series can have a profound influence on the observed bivariate coincidence rates. To control for these effects and assess the statistical significance of the computed coincidence rates r we create 1000 iAAFT (iterative Amplitude Adjusted Fourier Transformation, Schreiber and Schmitz, 2000; Venema et al., 2006) surrogate time series for each site and grid cell. The iAAFT surrogates are fully statistically independent from the original time series, but characterized by the same amplitude distribution and most importantly, the same autocorrelation properties. Hence, we can investigate what would be the coincidence rate of extremes that we would expect to arise by chance between two time series of a given autocorrelation structure. We calculate for each site and grid cell the distribution of the coincidence rates of the iAAFT surrogate time series. The coincidence rate r (calculated from climate and biotic extremes) is assumed to be significant, if it is higher than the 90 % percentile of the surrogate distribution. In the following analysis, we only consider TRW sites and simulated grid cells with a significant coincidence rate r. For brevity, these locations are in the following addressed as significant sites or grid cells.

2.4 Detection of European-wide extreme years

To identify years with a pronounced European wide forest response to climate extremes, i.e. years that yield a high number of coincidences occurs across the continent, we take the sum over all coincidences at significant sites/grid cells occurring during a specific year and divide it by the number of all significant sites/grid cells, again yielding a number between 0 and 1 (0 if no coincidences occur at significant sites/grid cells and 1 if all significant sites show a coincidence in the year considered). As "European-wide extreme years" we define all values one standard deviation above the average annual significant coincidence rate.

3 Results and discussion

In the following we first discuss the general picture of the impact of climate extremes on measured TRW and modeled NPP and then focus on patterns of spatial and temporal coincidence rates at significant sites/grid cells.

3.1 Down-regulation of forest growth by extreme events

To estimate potential effects of extreme events on tree growth and productivity, we evaluated deviations of TRW and simulated NPP during climatically attributable extreme years from growth responses in average climate years. 16 % (53 %) and 13 % (53 %) of the TRW values are below two (one) standard deviations in years with extremely high temperatures and low precipitation, respectively (Fig. 2a and b). At TRW sites, 30 % and 26 % (79 % and 73 %) of simulated NPP values are below two (one) standard deviations in years with precipitation and temperature extremes, respectively (Fig. 2c and d). The stronger reduction in NPP compared to TRW may partially reflect the fact that the same climate forcing data are used to drive simulated NPP (i.e. a higher probability for coincidences between climate and NPP extremes than coincidences between climate and TRW extremes). The stronger reduction in NPP compared to TRW shows also that responses in TRW may be buffered, e.g. by stored carbohydrates (Carbone et al., 2013; Dietze et al., 2013; Richardson et al., 2013) and responses may not or only be seen in the years after the extreme event. In contrast to that, the short-term carbon storage product NPP responds rather instantly to extreme events. Our definition of extremes additionally neglects any impacts of extreme events that occur outside the growing season which could have significant impact on forest productivity such as respiratory carbon losses in autumn and winter depleting carbon storage pools and reduce growth in the next year (e.g. Piao et al., 2008). Extremely warm temperatures in winter may also increase the snow amount in the boreal zone leading to a delayed start of the next growing season (Helama et al., 2013). In contrast to that, warm winter/spring temperatures are beneficial for an earlier start of the next growing season

(Polgar and Primack, 2011). This aggregated picture (Fig. 2) suggests that TRW and simulated NPP show subtle differences in their response to climate extremes and that the seasonality of climate anomalies may be of vital importance in this respect. Hence, an in-depth investigation as to how these differences can be attributed and to what extent TRW can be used to benchmark dynamic vegetation models for responses to extreme events is necessary.

3.2 Extreme years as determined from coincidences across Europe

To analyze responses of forest growth to drought and heat extremes found in models and observations, it is necessary to first evaluate whether the timings of the climate driven reductions in TRW and simulated NPP events match reasonably well. In this context, we determine European-wide extreme years as described in Sect. 2.4. For both, TRW and simulated NPP, we identify the years 1911, 1921, 1945, 1947, 1976 and 2003 (Fig. 3, dark grey boxes) as dry extremes with substantial biotic impacts. Extreme years with high temperatures are detected in 1934, 1945, 1947, 1949, 1950, 2002 and 2003 (Fig. 3). These results are in good agreement with earlier studies which identified events during these years. Babst et al. (2012) show in their analysis that 1947 had extremely low growth in southern and southeastern and Central Europe due to dry conditions. Neuwirth et al. (2007) reveal 1921 as negative extreme year in Rhone-valley, Jura, Northern Bavaria, Northern Germany and 1947 as negative extreme year in Western Poland, Northwestern Germany and Slovenia. Battipaglia et al. (2010) reconstructed temperature extremes from tree rings and found extremely warm conditions in 1911, 1921, 1964 and 2003. Extreme fire years are reported in 1947 and 1976 in Germany (Goldammer, 2001). The effects of the extreme year 2003 in Europe are well known (e.g. Ciais et al., 2005). Thus, we demonstrate the possibility to identify European-wide extreme years regarding heat and drought based on our coincidence analysis.

3.3 Spatial distribution of responses to extreme events

In a next step, we focus on the regional patterns of biotic responses revealed by coincidence analysis. The value of tree ring records as model benchmarks under climate extremes will crucially depend on the matches in these spatial patterns. Figure 4 identifies areas where simulated NPP of broadleaved and needleleaved trees show significant coincidences with precipitation and temperature extremes, respectively. Analogously, Fig. 5 shows this picture for TRW. The predominant pattern is that we find more significant grid cells with high coincidence rates between simulated NPP and precipitation (n = 259 at grid cells with TRW site) than with temperature extremes (n = 74 at grid cells with TRW site; Fig. 4) during the growing season, which may be related to an overestimation of the modeled P sensitivity of NPP (Babst et al., 2013b; Beer et al., 2010). It also shows that water is an important driving factor at many sites particularly under extreme conditions (Reichstein et al., 2013; Zscheischler et al., 2014b). Drought conditions may of course not only be inferred from a lack of rainfall but also from temperature, which in dry areas, e.g. the Mediterranean region, drives the vapor pressure deficit (Williams et al., 2012). For observed TRW we find almost the same amount of significant sites for coincidences with P (n = 189) as for coincidences with T (n = 139; Fig. 5). In contrast to observed TRW, simulated NPP displays generally low or insignificant coincidence rates with high temperature and low precipitation extremes in mountainous areas (Figs. 4 and 5). This may be due to the mean climatology covered in the respective grid cell resolution which does not reflect climatic differences along steep elevational gradients in the Alps and the related responses which are displayed by TRW (e.g. King et al., 2013). Due to this fact, these factors in their extremes (high temperatures, low precipitation) are not limiting simulated NPP during the growing season in this region. Thus, for correctly representing site-climate, and particularly site-level climate extremes, data from climate stations at the sites (of which only very few, and of a limited time span, are available) would be ideal. This highlights the importance of developing higher resolution long-term climate datasets based on downscaling to local site conditions.

Zonal patterns become more obvious from binning of results (Fig. 6). For both, simulated and observed growth responses, we find a $\sim$ 40 percent probability that a climatic extreme is associated with a biotic extreme, i.e. reduced growth response in the current or subsequent year. The simulated NPP at tree ring sites displays an increase in the coincidence rate r along a mean annual temperature gradient with lower r in low temperature zones and higher r in high temperature zones (Fig. 6, blue dots). The coincidence rates between simulated NPP and P range between $r \approx 0.38$ to 0.54 (Fig. 6a), whereas for NPP and T they scatter around ~ 0.4 (Fig. 6b). Also here, the overestimation of the P sensitivity of simulated NPP in comparison to TRW is visible. TRW displays rather constant coincidence rates of ~ 0.4 with T (Fig. 6a, red dots) and P (Fig. 6b) along the temperature gradient. The lower coincidence rates in TRW may be driven by adverse effects of extreme T, e.g. in mountainous areas, where high temperatures during the growing season may even lead to increased growth (Jolly et al., 2005). Also, the importance of non-structural carbohydrates (NSCs) should not be underestimated. NSCs can be stored up to 10 yr, used as resources during unfavourable growth conditions, and thus buffer the effect of extreme events (e.g. Carbone et al., 2013; Richardson et al., 2013).

3.4 Instantaneous and lagged responses to extreme events

To further assess responses in tree-growth to climate extremes found in models and observations, we need to analyze the dynamics of biotic responses to climatic extremes. Therefore, we compare the coincidence rate r in the same year (i.e. instantaneous effects, calculated with Δt = 1 and tau = 0) with the coincidence rate in the year after the climate extreme (i.e. lagged effects, calculated with Δt = 1 and tau = 1, Fig. 7 and see also Fig. 1). In TRW there appears to be a higher number of coincidences in the year after the extreme compared to the instantaneous response, thus the response of tree rings to climate extremes seems to be lagged, mainly in response to extreme drought

(Fig. 7, upper row). Hence, we can confirm that negative precipitation anomalies combined with positive temperature extremes lead to reduced growth not only in the current but also in the following year. Similarly, other studies (e.g. Babst et al., 2012; Franke et al., 2013) have emphasized the importance of considering lagged effects in measured TRW. Babst et al. (2012) found that particularly late growing season extremes lead to reduced forest productivity in the following year. Another important finding is that this behavior is not as strong in simulated NPP (Fig. 7, lower rows). In the model, lagged effects in NPP are simulated when unfavorable climate conditions lead to low productivity and high respiration costs during the current year and thus less accumulation of biomass. Constant or less accumulated biomass then leads to reduced NPP during the following year. Since NPP represents a rather short-term measure of carbon use compared to TRW, it thus responds more instantaneously to changes in photosynthesis and respiration during extreme events. In contrast, TRW integrates carbon accumulation and growth over a whole growing season, relies in part on stored carbohydrates, and may even be influence by longer-term response to canopy and root architecture. These considerations may explain why TRW may therefore not react in a similar way as NPP to extreme events.

4 Conclusions

We present a simple method for detecting impacts of extreme events in time series of climate and forest growth that is based on coincidence analysis. The coincidence metric can be seen as a "unit-free" neutral measure for biotic responses to climate impacts. The method is general and independent of units, so that we do not have to, e.g., convert tree ring width to NPP for comparison with model output; instead we can compare the results of the coincidence analysis to test for possible causal relationships between extreme climate and extreme growth responses. These methods are particularly suitable for the analysis of extreme events since they are not based on correlations but on coincidences of events in time series.

Tree rings are long-term observational time series related to forest productivity and are thus valuable archives for improving our process-understanding of forest responses to extreme events and thus, for evaluating dynamic vegetation models. Our study shows that high temperature and low precipitation extremes lead to substantial losses in forest productivity, which is 50 to 80 % below one standard deviation during extreme years. Based on the coincidence analysis, we are able to quantify for the first time the probability that a climate extreme triggers an extreme reaction in the terrestrial biosphere (e.g., ~ 40 % for T extremes in both TRW and modeled NPP, and 40 vs. 60 % for P extremes). We identified years with climate extremes which caused extreme ecosystem responses in Europe for the 20th century, which are consistent with previously reported evidence.

From our comparison of observed and modeled data, we conclude that (a) the impact of heat and drought on European forest ecosystems is severe, (b) to improve our understanding of related processes, very high resolution long-term climate data at site level are needed, (c) process-based models should be improved for site-specific applications by improving the representation of processes related to lag effects (e.g. storage of non-structural carbon and monthly allocation). Since most general dynamic vegetation models are developed for rather "average" conditions, the representation of responses to extreme events has to be improved for a better understanding of e.g. the long-term fate of the European carbon balance.

Acknowledgements. This work emerged from the CARBO-Extreme project (grant agreement no. 226701) of the European Community's 7th framework program. We thank all data producers for contributing their TRW data to the ITRDB. MDM acknowledges support by the GEOCARBON project (grant agreement no: 283080) of the European Community's 7th framework program. JFD thanks the German National Academic Foundation and the Stordalen Foundation for financial support. FB acknowledges funding from the Swiss National Science Foundation (grant PBSKP2_144034).

References

Andreu-Hayles, L., Planells, O., Gutierrez, E., Muntan, E., Helle, G., Anchukaitis, K. J., and Schleser, G. H.: Long tree-ring chronologies reveal 20th century increases in water-use efficiency but no enhancement of tree growth at five Iberian pine forests, Glob. Change Biol., 17, 2095–2112, doi:10.1111/j.1365-2486.2010.02373.x, 2011.

Babst, F., Carrer, M., Poulter, B., Urbinati, C., Neuwirth, B., and Frank, D.: 500 yr of regional forest growth variability and links to climatic extreme events in Europe, Environ. Res. Lett., 7, 045705, doi:10.1088/1748-9326/7/4/045705, 2012.

Babst, F., Bouriaud, O., Papale, D., Gielen, B., Janssens, I. A., Nikinmaa, E., Ibrom, A., Wu, J., Bernhofer, C., Koestner, B., Gruenwald, T., Seufert, G., Ciais, P., and Frank, D.: Above-ground woody carbon sequestration measured from tree rings is coherent with net ecosystem productivity at five eddy-covariance sites, New Phytol., 201, 1289–1303, 2013a.

Babst, F., Poulter, B., Trouet, V., Tan, K., Neuwirth, B., Wilson, R., Carrer, M., Grabner, M., Tegel, W., Levanic, T., Panayotov, M., Urbinati, C., Bouriaud, O., Ciais, P., and Frank, D.: Site- and species-specific responses of forest growth to climate across the European continent, Global Ecol. Biogeogr., 22, 706–717, doi:10.1111/geb.12023, 2013b.

Barriopedro, D., Fischer, E. M., Luterbacher, J., Trigo, R., and Garcia-Herrera, R.: The hot summer of 2010: redrawing the temperature record map of Europe, Science, 332, 220–224, doi:10.1126/science.1201224, 2011.

Battipaglia, G., Frank, D., Büntgen, U., Dobrovolny, P., Bradzdil, R., Pfister, C., and Esper, J.: Five centuries of Central European temperature extremes reconstructed from tree-ring density and documentary evidence, Global Planet. Change, 72, 182–191, 2010.

Beer, C., Reichstein, M., Tomelleri, E., Ciais, P., Jung, M., Carvalhais, N., Rödenbeck, C., Arain, M. A., Baldocchi, D., Bonan, G. B., Bondeau, A., Cescatti, A., Lasslop, G., Lindroth, A., Lomas, M., Luyssaert, S., Margolis, H., Oleson, K. W., Roupsard, O., Veenendaal, E., Viovy, N., Williams, C., Woodward, F. I., and Papale, D.: Terrestrial gross carbon dioxide uptake: global distribution and covariation with climate, Science, 329, 834–838, 2010.

Bondeau, A., Smith, P. C., Zaehle, S., Schaphoff, S., Lucht, W., Cramer, W., Gerten, D., Lotze-Campen, H., Müller, C., Reichstein, M., and Smith, B.: Modelling the role of agriculture for the 20th century global terrestrial carbon balance, Glob. Change Biol., 13, 679–706, 2007.

Bréda, N., Huc, R., Granier, A., and Dreyer, E.: Temperate forest trees and stands under severe drought: a review of ecophysiological responses, adaptation processes and long-term consequences, Ann. For. Sci., 63, 625–644, 2006.

Carbone, M. S., Czimczik, C. I., Keenan, T., Murakami, P., Pederson, N., Schaberg, P. G., Xu, X., and Richardson, A. D.: Age, allocation and availability of nonstructural carbon in mature red maple trees, New Phytol., 200, 1145–1155, 2013.

Ciais, P., Reichstein, M., Viovy, N., Granier, A., Ogée, J., Allard, V., Aubinet, M., Buchmann, N., Bernhofer, C., Carrara, A., Chevallier, F., De Noblet, N., Friend, A. D., Friedlingstein, P., Grünwald, T., Heinesch, B., Keronen, P., Knohl, A., Krinner, G., Loustau, D., Manca, G., Matteucci, G., Miglietta, F., Ourcival, J. M., Papale, D., Pilegaard, K., Rambal, S., Seufert, G., Soussana, J. F., Sanz, M. J., Schulze, E.-D., Vesala, T., and Valentini, R.: Europe-wide reduction in primary productivity caused by the heat and drought in 2003, Nature, 437, 529–533, 2005.

Cook, E. R. and Peters, K.: Calculating unbiased tree-ring indices for the study of climatic and environmental change, The Holocene, 7, 361–370, 1997.

Cotrufo, M. F., Alberti, G., Inglima, I., Marjanović, H., LeCain, D., Zaldei, A., Peressotti, A., and Miglietta, F.: Decreased summer drought affects plant productivity and soil carbon dynamics in a Mediterranean woodland, Biogeosciences, 8, 2729–2739, doi:10.5194/bg-8-2729-2011, 2011.

Dalmonech, D. and Zaehle, S.: Towards a more objective evaluation of modelled land-carbon trends using atmospheric CO_2 and satellite-based vegetation activity observations, Biogeosciences, 10, 4189–4210, doi:10.5194/bg-10-4189-2013, 2013.

Dee, D. P., Uppala, S. M., Simmons, A. J., Berrisford, P., Poli, P., Kobayashi, S., Andrae, U., Balmaseda, M. A., Balsamo, G., Bauer, P., Bechtold, P., Beljaars, A. C. M., van de Berg, L., Bidlot, J., Bormann, N., Delsol, C., Dragani, R., Fuentes, M., Geer, A. J., Haimberger, L., Healy, S. B., Hersbach, H., Holm, E. V., Isaksen, L., Kallberg, P., Kohler, M., Matricardi, M., McNally, A. P., Monge-Sanz, B. M., Morcrette, J. J., Park, B. K., Peubey, C., de Rosnay, P., Tavolato, C., Thepaut, J. N., and Vitart, F.: The ERA-Interim reanalysis: configuration and performance of the data assimilation system, Q. J. Roy. Meteor. Soc., 137, 553–597, doi:10.1002/qj.828, 2011.

Dietze, M. C., Sala, A., Carbone, M. S., Czimczik, C. I., Mantooth, J. A., Richardson, A. D., and Vargas, R.: Nonstructural carbon in woody plants, Annu. Rev. Plant Biol., 65, 2013.

Donges, J. F., Donner, R. V., Trauth, M. H., Marwan, N., Schellnhuber, H. J., and Kurths, J.: Nonlinear detection of paleoclimate-variability transitions possibly related to human evolution, P. Natl. Acad. Sci. USA, 108, 20422–20427, doi:10.1073/pnas.1117052108, 2011.

Farquhar, G. D., von Caemmerer, S., and Berry, J. A.: A biochemical model of photosynthesic CO_2 assimilation in leaves of C3 plants, Planta, 149, 78–90, 1980.

Field, C. B., Barros, V., Stocker, T. F., and Dahe, Q.: Special Report on Managing the risks of Extreme Events and Disasters to Advance Climate Change Adaptation (SREX), Cambridge University Press, 2012.

Frank, D., Esper, J., and Cook, E.: Adjustment for proxy number and coherence in large-scale temperature reconstruction, Geophys. Res. Lett., 34, L16709, doi:10.1029/2007GL030571, 2007.

Franke, J., Frank, D., Raible, C. C., Esper, J., and Brönnimann, S.: Spectral biases in tree-ring climate proxies, Nature Climate Change, 3, 360–364, 2013.

Fritts, H. C.: Tree Rings and Climate, Academic Press, London, 1976.

Gedalof, Z. and Berg, A. A.: Tree ring evidence for limited direct CO_2 fertilization of forests over the 20th century, Global Biogeochem. Cy., 24, 6, Gb3027, doi:10.1029/2009gb003699, 2010.

Gerten, D., Schaphoff, S., Haberlandt, U., Lucht, W., and Sitch, S.: Terrestrial vegetation and water balance – hydrological evaluation of a dynamic global vegetation model, J. Hydrol., 286, 249–270, 2004.

Goldammer, J. G.: International Forest Fire News, Joint FAO/ECE/ILO Committee on Forest Technology, Management and Training and its secretariat, the Timber Section, UN-ECE Trade Division, Geneva, 103, 2001.

Granier, A., Reichstein, M., Bréda, N., Janssens, I. A., Falge, E., Ciais, P., Grünwald, T., Aubinet, M., Berbigier, P., Bernhofer, C., Buchmann, N., Facini, O., Grassi, G., Heinesch, B., Illvesniemi, H., Keronen, P., Knohl, A., Köstner, B., Lagergren, F., Lindroth, A., Longdoz, B., Loustau, D., Mateus, J., Montagnani, L., Nyst, C., Moors, E., Papale, D., Pfeiffer, M., Pilegaard, K., Pita, G., Pumpanen, J., Rambal, S., Rebmann, C., Rodrigues, A., Seufert, G., Tenhunen, J. D., Vesala, T., and Wang, Q.: Evidence for soil water control on carbon and water dynamics in European forests during the extremely dry year: 2003, Agr. Forest Meteorol., 143, 123–145, 2007.

Hanewinkel, M., Cullmann, D., Schelhaas, M.-J., Nabuurs, G. J., and Zimmermann, N. E.: Climate change may cause severe loss in the economic value of European forest land, Nature Clim. Change, 3, 203–207, 2013.

Haxeltine, A. and Prentice, I. C.: A general model for the light-use efficiency of primary production, Funct. Ecol., 10, 551–561, 1996.

Helama, S., Mielikäinen, K., Timonen, M., Herva, H., Tuomenvirta, H., and Venäläinen, A.: Regional climatic signals in Scots pine growth with insights into snow and soil associations, Dendrobiology, 70, 27–34, 2013.

Innes, J. L.: The impact of climatic extreme on forest: an introduction, in: The Impacts of Climate Variability on Forests (Lecture Notes in Earth Sciences), edited by: Beniston, M. and Innes, J. L., Springer, Berlin, 1–18, 1998.

Janssen, I. A., Freibauer, A., Ciais, P., Smith, P., Nabuurs, G. J., Folberth, P., Schlamadinger, B., Hutjes, R. W. A., Ceulemans, R., Schulze, E.-D., Valentini, R., and Dolman, A. J.: Europe's terrestrial biosphere absorbs 7 to 12 % of European anthropogenic CO_2 emissions, Science, 300, 1538–1542, 2003.

Jentsch, A., Kreyling, J., Elmer, M., Gellesch, E., Glaser, B., Grant, K., Hein, R., Lara Jimenez, M., Mirzaee, H., Nadler, S., Nagy, L., Otieno, D., Pritsch, K., Rascher, U., Schädler, M., Schloter, M., Singh, A., Stadler, J., Walter, J., Wellstein, C., Wöllecke, J., and Beierkuhnlein, C.: Climate extremes initiate ecosystem regulating functions while maintaining productivity, J. Ecol., 99, 689–702, 2011.

Jolly, W. M., Dobbertin, M., Zimmermann, N. E., and Reichstein, M.: Divergent vegetation growth responses to the 2003 heat wave in the Swiss Alps, Geophys. Res. Lett., 32, L18409, doi:10.1029/2005GL023252, 2005.

Keenan, T. F., Baker, I., Barr, A., Ciais, P., Davis, K., Dietze, M., Dragon, D., Gough, C. M., Grant, R., Hollinger, D., Hufkens, K., Poulter, B., McCaughey, H., Raczka, B., Ryu, Y., Schaefer, K., Tian, H. Q., Verbeeck, H., Zhao, M. S., and Richardson, A. D.: Terrestrial biosphere model performance for inter-annual variability of land-atmosphere CO_2 exchange, Glob. Change Biol., 18, 1971–1987, doi:10.1111/j.1365-2486.2012.02678.x, 2012.

Keenan, T. F., Hollinger, D. Y., Bohrer, G., Dragoni, D., Munger, J. W., Schmid, H. P., and Richardson, A. D.: Increase in forest water-use efficiency as atmospheric carbon dioxide concentrations rise, Nature, 499, 324–327, doi:10.1038/nature12291, 2013.

Kelley, D. I., Prentice, I. C., Harrison, S. P., Wang, H., Simard, M., Fisher, J. B., and Willis, K. O.: A comprehensive benchmarking system for evaluating global vegetation models, Biogeosciences, 10, 3313–3340, doi:10.5194/bg-10-3313-2013, 2013.

King, G. M., Gugerli, F., Fonti, P., and Frank, D.: Tree growth response along an elevational gradient: climate or genetics?, Oecologia, 173, 1587–1600, 2013.

Kuptz, D., Fleischmann, F., Matyssek, R., and Grams, T.: Seasonal patterns of carbon allocation to respiratory pools in 60-yr-old deciduous (*Fagus sylvatica*) and evergreen (*Picea abies*) trees assessed via whole-tree stable carbon isotope labeling, New Phytol., 191, 160–172, 2011.

Lindner, M., Maroschek, M., Netherer, S., Kremer, A., Barbati, A., Garcia-Gonzalo, J., Seidl, R., Delzon, S., Corona, P., Kolstrom, M., Lexer, M. J., and Marchetti, M.: Climate change impacts, adaptive capacity, and vulnerability of European forest ecosystems, Forest Ecol. Manag., 259, 698–709, doi:10.1016/j.foreco.2009.09.023, 2010.

Luo, Y. Q., Randerson, J. T., Abramowitz, G., Bacour, C., Blyth, E., Carvalhais, N., Ciais, P., Dalmonech, D., Fisher, J. B., Fisher, R., Friedlingstein, P., Hibbard, K., Hoffman, F., Huntzinger, D., Jones, C. D., Koven, C., Lawrence, D., Li, D. J., Mahecha, M., Niu, S. L., Norby, R., Piao, S. L., Qi, X., Peylin, P., Prentice, I. C., Riley, W., Reichstein, M., Schwalm, C., Wang, Y. P., Xia, J. Y., Zaehle, S., and Zhou, X. H.: A framework for benchmarking land models, Biogeosciences, 9, 3857–3874, doi:10.5194/bg-9-3857-2012, 2012.

Moreno, J. M., Torres, I., Luna, B., Oechel, W. C., and Keeley, J. E.: Changes in fire intensity have carry-over effects on plant responses after the next fire in southern California chaparral, J. Veg. Sci., 24, 395–404, 2013.

Mund, M., Kutsch, W., Wirth, C., Kahl, T., Knohl, A., Skomarkova, M., and Schulze, E. D.: The influence of climate and fructification on the inter-annual variability of stem growth and net primary productivity in an old-growth, mixed beech forest, Tree Physiol., 30, 689–704, 2010.

Neuwirth, B., Schweingruber, F. H., and Winigera, M.: Spatial patterns of central European pointer years from 1901 to 1971, Dendrochronologia, 24, 79–89, 2007.

Norby, R. J., Warrena, J. M., Iversena, C. M., Medlyn, B. E., and McMurtrie, R. E.: CO_2 enhancement of forest productivity constrained by limited nitrogen availability, P. Natl. Acad. Sci. USA, 107, 19368–19373, 2010.

Penuelas, J., Canadell, J., and Ogaya, R.: Increased water-use efficiency during the 20th century did not translate into enhanced tree growth, Global Ecol. Biogeogr., 20, 597–608, 2011.

Piao, S., Ciais, P., Friedlingstein, P., Peylin, P., Reichstein, M., Luyssaert, S., Margolis, H., Fang, J., Barr, A., Chen, A., Grelle, A., Hollinger, D. Y., Laurila, T., Lindroth, A., Richardson, A. D., and Vesala, T.: Net carbon dioxide losses of northern ecosystems in response to autumn warming, Nature, 451, 49–53, 2008.

Pinty, B., Clerici, M., Andredakis, I., Kaminski, T., Taberner, M., Verstraete, M. M., Gobron, N., Plummer, S., and Widlowski, J.-L.: Exploiting the MODIS albedos with the two-stream inversion package (JRC-TIP) part II: fractions of transmitted and absorbed fluxes in the vegetation and soil layers, J. Geophys. Res.-Atmos., 116, D09106, doi:10.1029/2010JD015373, 2011.

Polgar, C. and Primack, R. B.: Leaf-out phenology of temperate woody plants: from trees to ecosystems, New Phytol., 191, 926–941, 2011.

Reichstein, M., Bahn, M., Ciais, P., Frank, D., Mahecha, M. D., Seneviratne, S. I., Zscheischler, J., Beer, C., Buchmann, N., Frank, D. C., Papale, D., Rammig, A., Smith, P., Thonicke, K., van der Velde, M., Vicca, S., Walz, A., and Wattenbach, M.: Climate extremes and the carbon cycle, Nature, 500, 287–295, 2013.

Reyer, C. P. O., Leuzinger, S., Rammig, A., Wolf, A., Bartholomeus, R. P., Bonfante, A., De Lorenzi, F., Dury, M., Gloning, P., Abou Jaoudé, R., Klein, T., Kuster, T. M., Martins, M., Niedrist, G., Riccardi, M., Wohlfahrt, G., De Angelis, P., de Dato, G., François, L., Menzel, A., and Pereira, M.: A plant's perspective of extremes: terrestrial plant responses to changing climatic variability, Glob. Change Biol., 19, 75–89, 2012.

Richardson, A. D., Carbone, M. S., Keenan, T., Czimczik, C. I., Hollinger, D. Y., Murakami, P., Schaberg, P. G., and Xu, X.: Seasonal dynamics and age of stemwood nonstructural carbohydrates in temperate forest trees, New Phytol., 197, 850–861, 2013.

Schreiber, T. and Schmitz, A.: Surrogate time series, Physica D, 142, 346–382, 2000.

Schwalm, C., Williams, C. A., Schaefer, K., Baldocchi, D., Black, T. A., Goldstein, A. H., Law, B. E., Oechel, W., Tha Paw, U. K., and Scott, R. L.: Reduction in carbon uptake during turn of the century drought in western North America., Nat. Geosci., 5, 551–556, 2012.

Sitch, S., Smith, B., Prentice, I. C., Arneth, A., Bondeau, A., Cramer, W., Kaplans, J. O., Levis, S., Lucht, W., Sykes, M. T., Thonicke, K., and Venevsky, S.: Evaluation of ecosystem dynamics, plant geography and terrestrial carbon cycling in the LPJ dynamic global vegetation model, Glob. Change Biol., 9, 161–185, 2003.

Smith, M. D.: An ecological perspective on extreme climatic events: a synthetic definition and framework to guide future research, J. Ecol., 99, 656–663, 2011.

Thonicke, K., Spessa, A., Prentice, I. C., Harrison, S. P., Dong, L., and Carmona-Moreno, C.: The influence of vegetation, fire spread and fire behaviour on biomass burning and trace gas emissions: results from a process-based model, Biogeosciences, 7, 1991–2011, doi:10.5194/bg-7-1991-2010, 2010.

Venema, V., Bachner, S., Rust, H. W., and Simmer, C.: Statistical characteristics of surrogate data based on geophysical measurements, Nonlin. Processes Geophys., 13, 449–466, doi:10.5194/npg-13-449-2006, 2006.

Weedon, G. P., Gomes, S., Viterbo, P., Shuttleworth, W. J., Blyth, E., Osterle, H., Adam, J. C., Bellouin, N., Boucher, O., and Best, M.: Creation of the WATCH forcing data and its use to assess global and regional reference crop evaporation over land during the twentieth century, J. Hydrometeorol., 12, 823–848, doi:10.1175/2011jhm1369.1, 2011.

Wettstein, J. J., Littell, J. S., Wallace, J. M., and Gedalof, Z.: Coherent region-, species-, and frequency-dependent local climate signals in Northern Hemisphere tree-ring widths, J. Climate, 24, 5998–6012, 2011.

Williams, A. P., Allen, C. D., Macalady, A. K., Griffin, D., Woodhouse, C. A., Meko, D. M., Swetnam, T. W., Rauscher, S. A., Seager, R., Grissino-Mayer, H. D., Dean, J. S., Cook, E. R., Gangodagamage, C., Cai, M., and McDowell, N. G.: Temperature as a potent driver of regional forest drought stress and tree mortality, Nature Clim. Change, 3, 292–297, 2012.

Zscheischler, J., Mahecha, M., Harmeling, S., Rammig, A., Tomelleri, E., and Reichstein, M.: Extreme events in gross primary production: a characterization across continents, Biogeosciences Discuss., 11, 1869–1907, 2014a, http://www.biogeosciences-discuss.net/11/1869/2014/.

Zscheischler, J., Mahecha, M., Von Buttlar, J., Harmeling, S., Jung, M., Rammig, A., Randerson, J. T., Schöllkopf, B., Seneviratne, S. I., Tomelleri, E., Zaehle, S., and Reichstein, M.: Few extreme events dominate global interannual variability in gross primary production, Environ. Res. Lett., accepted, 2014b.

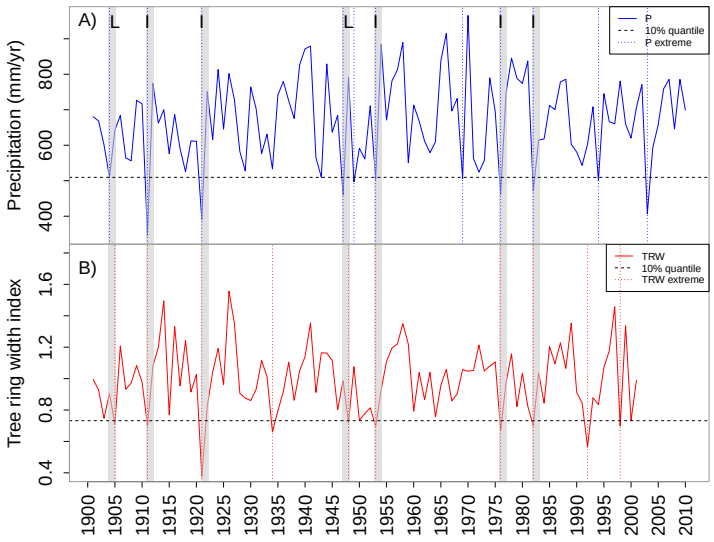

Fig. 1. Example for coincidence analysis between a time series of **(A)** precipitation (P) and **(B)** tree ring width indices (TRW). The dashed horizontal line represents the lower 10 % quantile. Events in precipitation or tree ring width that fall below this threshold are counted as extreme events, as indicated by the dotted vertical lines for P (blue) and TRW (red). Grey bars indicate the coincidence of extreme P and TRW events within a time window of two years ($\Delta t = 2$) and are counted as one coincidence. In this example, we count 11 climate extremes and 7 coincidences with TRW for $\Delta t = 2$, resulting in a coincidenced rate $r = 7/11 = 0.64$. Note that if there are two TRW extremes coinciding with one P extreme in the time window of $\Delta t = 2$, this would account for only one extreme. The letters "I" and "L" indicate instantaneous and lagged effects (i.e. carry-over effects), respectively. When setting the time window to $\Delta t = 1$ and tau = 0, five coincidences are counted and for $\Delta t = 1$ and tau = 1, two coincidences are counted in this example.

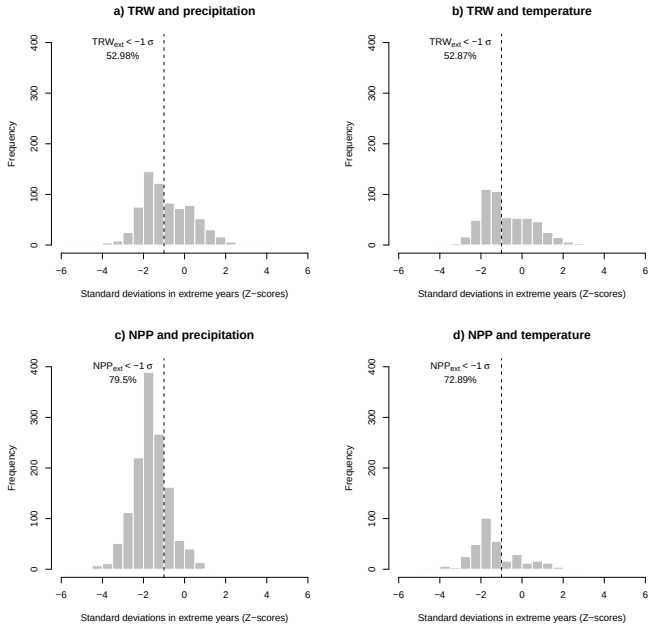

Fig. 2. Histograms of standard deviations of growth responses of TRW **(a, b)** and NPP **(c, d)** in extreme years (Z-scores). The vertical dashed grey line marks one negative standard deviation. Note that in the coincidence analysis for $\Delta t = 2$, deviations can also be positive since growth responses are accounted for in the year of the climate extreme. Thus, positive deviations indicate a positive growth response during the extreme year and a negative lagged response.

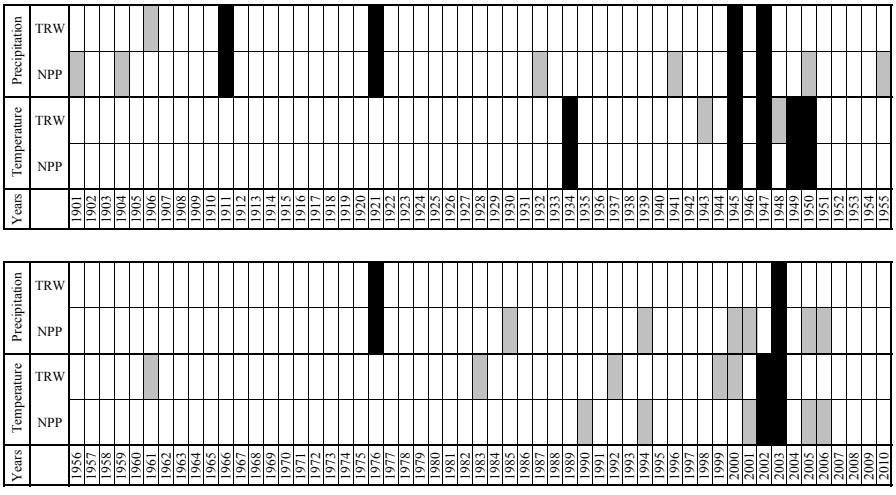

Fig. 3. Extreme years during the period 1901–2010 as detected by the coincidence analysis for TRW and NPP (only at TRW sites) with precipitation (upper two rows) and temperature (lower two rows). Dark grey bars indicate that extreme years were detected in TRW and in NPP.

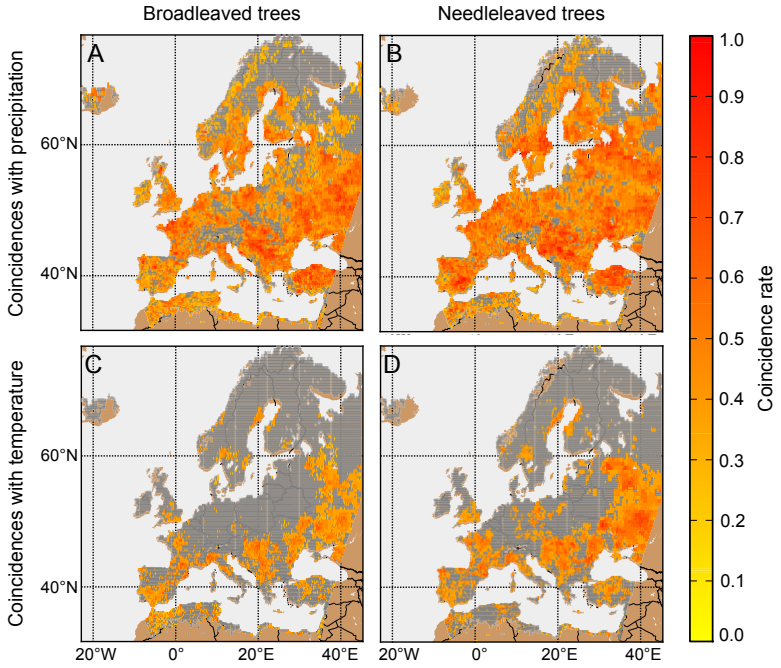

Fig. 4. Map of coincidence rates between extremes in simulated NPP and precipitation for **(A)** broadleaved and **(B)** needleleaved trees. Coincidence rates between extremes in simulated NPP and temperature for **(C)** broadleaved and **(D)** needle-leaved trees. The color bar gives the coincidence rate r for the coincidence analysis with $\Delta t = 2$. Only grid cells with significant coincidence rates are colored, non-significant grid cells are marked in grey. Note that the significance level for each grid cell is determined separately.

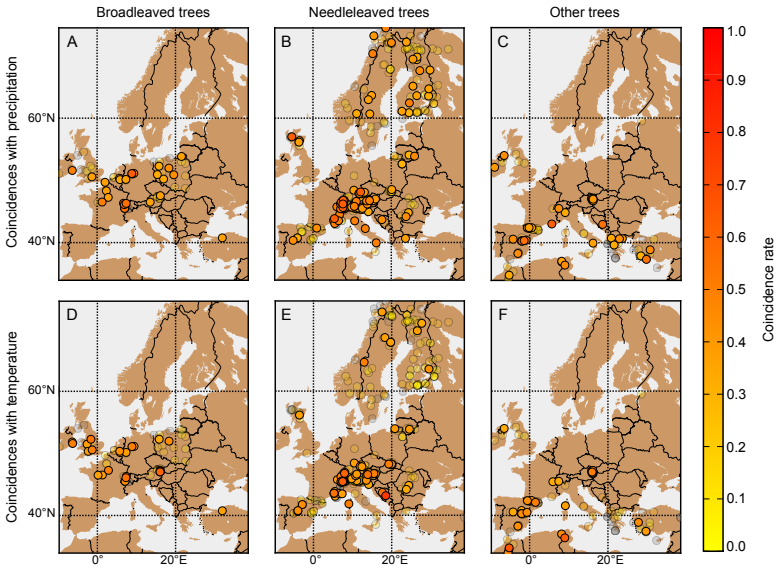

Fig. 5. Map of tree ring sites and coincidence rates at each site. Given are coincidence rates between extremes in TRW and precipitation for **(A)** broadleaved, **(B)** needleleaved and **(C)** other tree species. In the lower row, coincidence rates between extremes in TRW and temperature for **(D)** broadleaved, **(E)** needleleaved and **(F)** other tree species are displayed. Non-significant sites are marked in transparent colors. The color bar gives the coincidence rate r for the coincidence analysis with $\Delta t = 2$.

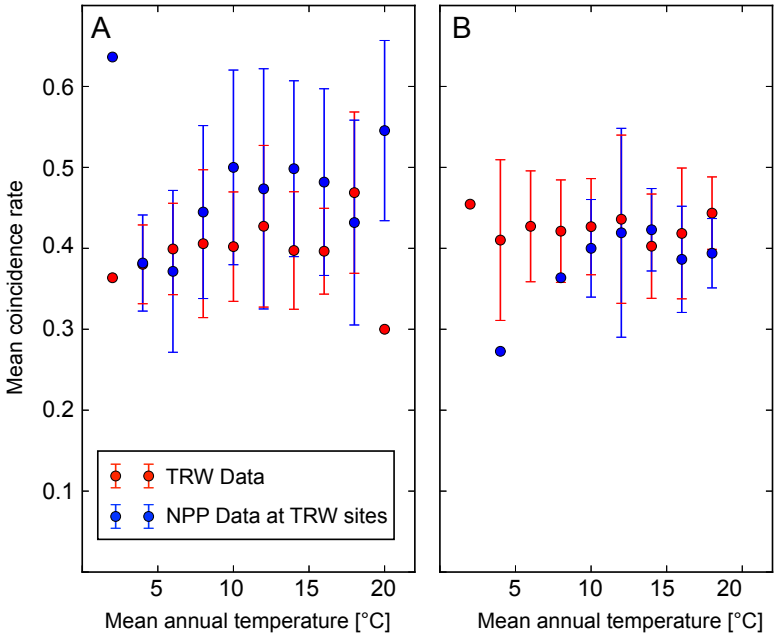

Fig. 6. Significant coincidence rates of TRW (red dots) and simulated NPP at TRW sites (blue dots) in climate space (as given in temperature classes, x-axis) averaged over all tree species. Sites/grid cells with significant coincidences are aggregated in 5 °C mean annual temperature classes. Error bars give the standard deviation among sites/grid cells. Note that for some bins, for TRW or site NPP only one value exists.

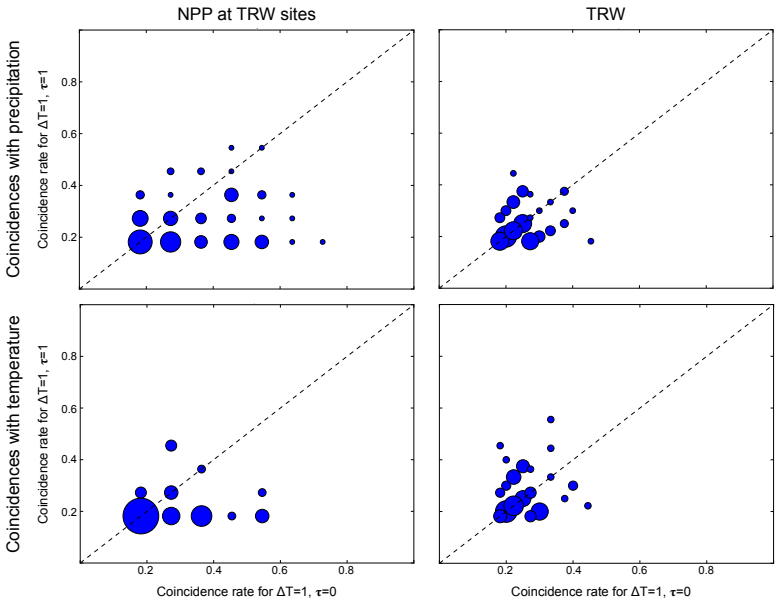

Fig. 7. Instantaneous (r calculated for $\Delta t = 1$ and tau = 0) vs. lagged (r calculated for $\Delta t = 1$ and tau = 1) coincidences of extreme events. The size of the dots is proportional to the amount of significant coincidences, i.e. larger dots indicate a higher number of sites/grid cells with significant coincidences. Note that the regular grid of coincidence rates results from consistent time series length for simulated NPP while the length of the time series for TRW differs.